

“Turn-On” Fluorescent Sensor for Hg<sup>2+</sup> via Displacement Approach

Guangjie He, Yonggang Zhao, Cheng He,\* Yang Liu, and Chunying Duan\*

State Key Laboratory of Fine Chemicals, Dalian University of Technology, Dalian, 116012, China

Received December 24, 2007

A new Cu<sup>2+</sup> compound Cu–NB, (where H<sub>2</sub>NB is bis(2-hydroxyl-naphthalene-carboxaldehyde) benzil dihydrazone) was synthesized as a highly selective fluorescence chemosensor for the detection of Hg<sup>2+</sup> in aqueous media through a displacement “turn-on” signaling strategy. Whereas the coordination of Cu<sup>2+</sup> resulted in a considerable quenching of the typical luminescence of the naphthol rings in Cu–NB, the addition of Hg<sup>2+</sup> ion led to a dramatic increase in the emission intensity of Cu–NB at about 530 nm (excitation at 430 nm). The competitive fluorescent experiments showed that alkali, alkaline earth metal ions, the group 12 metals Zn<sup>2+</sup>, Cd<sup>2+</sup>, the first-row transition-metal ions such as Mn<sup>2+</sup>, Fe<sup>2+</sup>, Co<sup>2+</sup>, and Ni<sup>2+</sup>, as well as Pb<sup>2+</sup> could not inhibit the Hg<sup>2+</sup>-binding fluorescent enhancement. It is postulated that the existence of Cu<sup>2+</sup> in the luminescent probe Cu–NB could turn away the interferences of other metal cations from Hg<sup>2+</sup> detection. The optical responses of the free ligand upon addition of Cu<sup>2+</sup> ion, and of the Hg–H<sub>2</sub>NB compound upon the addition of Cu<sup>2+</sup> were also investigated for comparisons.

## Introduction

Recently, the development of selective and sensitive imaging tools capable of rapidly monitoring heavy and transition metal ions (HTM), such as Pb<sup>2+</sup>, Cd<sup>2+</sup>, and Cu<sup>2+</sup>, ions has attracted considerable attention due to the environmental and biological relevance of such metal ions.<sup>1–4</sup> In this regard, the Hg<sup>2+</sup> ions is considered highly dangerous because the Hg<sup>2+</sup> ion is one of the environmentally most important metal ions whose toxicity, even at very low concentrations, has long been recognized and is a problem

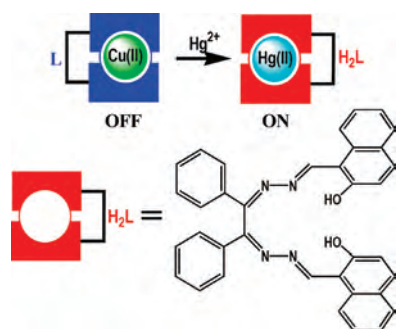
of primary concern.<sup>5</sup> Despite a reduction in its industrial use as a result of stricter regulations, high concentrations of mercury are still present in many environmental compartments, and it can still be found in many products of daily life such as paints, electronic equipment, and batteries.<sup>6,7</sup> These environmental and health problems have prompted the development of methods for the detection and the quantification of mercury applicability, especially in situations where conventional techniques are not appropriate. Small-molecule fluorescent chemosensors that selectively bind to and report on the target metal ion constitute one practical route toward this goal, and these probes showing fluorescence enhance-

\* To whom correspondence should be addressed. E-mail: cyduan@dlut.edu.cn.

- (1) (a) *Chemosensors of Ion and Molecule Recognition*, Desvergne, J. P., Czarnik, A. W., Eds.; Kluwer Academic Publishers: Dordrecht, The Netherlands, 1997. (b) Prodi, L.; Bolletta, F.; Montalti, M.; Zaccaroni, N. *Coord. Chem. Rev.* **2000**, *205*, 59–83.
- (2) (a) Liu, J.; Lu, Y. *J. Am. Chem. Soc.* **2003**, *125*, 6641–6642. (b) Chen, C.-T.; Huang, W.-P. *J. Am. Chem. Soc.* **2002**, *124*, 6246–6247. (c) Deo, S.; Godwin, H. A. *J. Am. Chem. Soc.* **2000**, *122*, 174–175.
- (3) (a) Choi, M.; Kim, M.; Lee, K. D.; Han, K.-N.; Yoon, I.-A.; Chung, H.-J.; Yoon, J. *Org. Lett.* **2001**, *3*, 3455–3457. (b) Marino, J. E.; Resendiz, J. C.; Disteldorf, N. H.; Fischer, S.; Stang, P. J. *Org. Lett.* **2004**, *6*, 651–653. (c) Bronson, R. T.; Michaelis, D. J.; Lamb, R. D.; Hussein, G. A.; Farnsworth, P. B.; Linford, M. R.; Izatt, R. M.; Bradshaw, J. S.; Savage, P. B. *Org. Lett.* **2005**, *7*, 1105–1108.
- (4) (a) Wu, Q.; Anslyn, E. V. *J. Am. Chem. Soc.* **2004**, *126*, 14682–14283. (b) Gunnlaugsson, T.; Leonard, J. P.; Murry, N. S. *Org. Lett.* **2004**, *6*, 1557–1560. (c) Mokhor, A.; Kramer, R. *Chem. Commun.* **2005**, 2244–2246. (d) Royzen, M.; Dai, Z.; Cannry, J. W. *J. Am. Chem. Soc.* **2006**, *127*, 1612–1613. (e) Xiang, Y.; Tong, A.; Jin, P.; Ju, Y. *Org. Lett.* **2006**, *8*, 2863–2866.

- (5) (a) Renzoni, A.; Zino, F.; Franchi, E. *Environ. Res., Sect. A* **1998**, *77*, 68–72. (b) Nendza, M.; Herbst, T.; Kussatz, C.; Gies, A. *Chemosphere* **1997**, *35*, 1875–1885. (c) Bolger, P. M.; Schwetz, B. A. *New Engl. J. Med.* **2002**, *347*, 1735–1736. (d) Harris, H. H.; Pickering, I. J.; George, G. N. *Science* **2003**, *301*, 1203. (e) Boening, D. W. *Chemosphere* **2000**, *40*, 1335–1351.
- (6) (a) U.S. EPA Regulatory Impact Analysis of the Clean Air Mercury Rule: EPA-452/R-05–003, Research Triangle Park, NC, 2005. (b) Clarkson, T. W.; Magos, L.; Myers, G. J. *New Engl. J. Med.* **2003**, *349*, 1731–1737. (c) Mottet, N. K.; Vahter, M. E.; Charleston, J. S.; Friberg, L. T. *Met. Ions Biol. Syst.* **1997**, *34*, 371–403. (d) Davidson, P. W.; Myers, G. J.; Cox, C.; Axtell, C.; Shamlaye, C.; Sloane-Reeves, J.; Cernichiari, E.; Needham, L.; Choi, A.; Wang, Y.; Berlin, M.; Clarkson, T. W. *J. Am. Med. Assoc.* **1998**, *280*, 701–707. (e) Harada, M. *Crit. Rev. Toxicol.* **1995**, *25*, 1–24.
- (7) (a) Wang, Q. R.; Kim, D.; Dionysiou, D. D.; Sorial, G. A.; Timberlake, D. *Environ. Pollut.* **2004**, *131*, 323–336. (b) Dias, G. M.; Edwards, G. C. *Hum. Ecol. Risk Assess.* **2003**, *9*, 699–721.

**Scheme 1.** Potential Displacement Signaling Mechanism for Sensing  $\text{Hg}^{2+}$



ment as a result of the binding event are to be favored over those that exhibit fluorescence quenching upon cation complexation<sup>8</sup> (Scheme 1).

However, the design of sensors that give fluorescence enhancement upon  $\text{Hg}^{2+}$  binding is an intriguing challenge because  $\text{Hg}^{2+}$  like many other HTM cations is known as a fluorescent quencher.<sup>9,10</sup> In particular, one common limitation for heavy-metal detection in the environment is the low quantum efficiency of metal bound dyes in aqueous media compared to that in organic solvents. Consequently, the receptor molecules with fluorescent enhancements for  $\text{Hg}^{2+}$  need to be carefully designed so that the responsible mechanism for fluorescence quenching is maximized in the receptor and minimized in the metal-bound state of receptor.<sup>11,12</sup> On the basis of this design strategy, herein we describe a displacement approach for a  $\text{Hg}^{2+}$ -specific off-on fluorescence chemosensor. The  $\text{Cu}^{2+}$  coordination compound,  $\text{Cu-NB}$  ( $\text{H}_2\text{NB}$  = bis(2-hydroxyl-naphthalene-carboxaldehyde) benzil dihydrazone), exhibits a poor fluorescence (off state) due to the coordination of  $\text{Cu}^{2+}$  quenching the luminescence of the ligand. Upon the addition of the  $\text{Hg}^{2+}$  ions, the  $\text{Cu}^{2+}$  ion is displaced and a  $\text{Hg}^{2+}$  complex is formed, turning on the fluorescence (on state). Meanwhile, the coordination of  $\text{Cu}^{2+}$  in the metal-complexation chemosensor  $\text{Cu-NB}$  avoids the cross-sensitivities toward other metal ions, such as  $\text{Na}^+$ ,  $\text{K}^+$ ,  $\text{Mg}^{2+}$ ,  $\text{Ca}^{2+}$ , and the first-row transition metal ions.

## Experimental Section

**Materials and Measurements.** All chemicals used were of reagent grade or obtained from commercial sources and used without further purification except that the solvents for physical measurements were purified by classical methods. Elemental analyses (carbon, hydrogen, and nitrogen) were carried out on a PerkinElmer 240 analyzer. UV-vis spectra were obtained on a Shimadzu 3100 spectrophotometer at room temperature. <sup>1</sup>H NMR and <sup>13</sup>C NMR spectra were measured on a Bruker DRX-500 NMR spectrometer at room temperature. Differential pulse voltammetry results were recorded on an EG & G PAR model 273 instrument. The solution-state measurements were performed in a three-electrode cell with a pure argon gas inlet and outlet, which has a 50 ms pulse width with current samples 40 ms after the pulse was applied. A sweep rate of 20 mV s<sup>-1</sup> was used in all pulse experiments. The cell comprises a platinum wire working electrode, a platinum auxiliary electrode, and an Ag/AgCl wire reference electrode.

**Ligand H<sub>2</sub>NB.** A methanol solution of 2-hydroxy-1-naphthalene-carboxaldehyde (1.7g, 10 mmol) and benzil dihydrazone (1.2g, 5.0 mmol) were mixed and refluxed for 4 h. Yellow precipitates formed were filtered and washed with methanol and dried under vacuum. Yield: 73%. Crystals suitable for X-ray diffraction determination were obtained by slowly evaporating a dichloromethane solution of H<sub>2</sub>NB at room temperature. Anal. Calcd for C<sub>36</sub>H<sub>26</sub>N<sub>4</sub>O<sub>2</sub>: C, 79.1; H, 4.8; N, 10.3. Found: C, 79.3; H, 4.9; N, 10.1%. <sup>1</sup>H NMR (500 MHz, CDCl<sub>3</sub>): δ 12.57 (s, 2H, -OH), 9.74 (s, 2H, -CH=N-), 8.13 (d, 2H, Np), 8.00(d, 4H, Ph), 7.72(d, 2H, Np), 7.69(d, 2H, Np), 7.52(m, 4H, Ph), 7.48(m, 2H, Ph), 7.47(m, 2H, Np), 7.32 (t, 2H, Np), 7.03(d, 2H, Np). <sup>13</sup>C NMR (75 MHz, CDCl<sub>3</sub>), δ: 164.5, 160.8, 159.9, 134.9, 132.6, 131.8, 131.5, 129.1, 128.6, 127.8, 127.7, 127.2, 123.5, 121.4, 118.3, 108.3.

**Cu-NB.** A dichloromethane solution (15 mL) of H<sub>2</sub>NB (0.10 mmol, 0.055 g) and a methanol solution (15 mL) of Cu(ClO<sub>4</sub>)<sub>2</sub>·6H<sub>2</sub>O (0.10 mmol, 0.037 g) were mixed and refluxed for 3 h. A dark-red solid formed was filtered, washed with methanol (20 mL), and dried under vacuum. Yield: 80%. Crystals suitable for X-ray diffraction determination were obtained by slowly evaporating an ethanol/acetonitrile (1:1 v/v) solution of the copper compound at room temperature. Anal. Calcd for C<sub>36</sub>H<sub>24</sub>N<sub>4</sub>O<sub>2</sub>Cu·CH<sub>3</sub>CN: C, 70.4; H, 4.2; N, 10.8. Found: C, 70.3; H, 4.1; N, 10.9%.

**Hg-H<sub>2</sub>NB.** A dichloromethane solution (15 mL) of H<sub>2</sub>NB(0.10 mmol, 0.055 g) and the ethanol solution (15 mL) of Hg(ClO<sub>4</sub>)<sub>2</sub>·3H<sub>2</sub>O (0.10 mmol, 0.045 g) were mixed and refluxed for 3 h. A deep-orange solid formed was filtered, washed with methanol, and dried under vacuum. Yield: 82%. Anal. Calcd for C<sub>36</sub>H<sub>26</sub>N<sub>4</sub>O<sub>10</sub>HgCl<sub>2</sub>·C<sub>2</sub>H<sub>5</sub>OH: C, 46.0; H, 3.2; N, 5.6; Found: C, 46.3; H, 3.1; N, 5.8%. <sup>1</sup>H NMR (500 MHz, CDCl<sub>3</sub>), δ: 12.90 (broad, 2H, -OH) 9.84 (s, 2H, -CH=N-), 8.19 (d, 2H, Np), 8.04(d, 4H, Ph), 7.96(d, 2H, Np), 7.69(d, 2H, Np), 7.63(m, 4H, Ph), 7.57(m, 2H, Ph), 7.54 (m, 2H, Np), 7.42 (t, 2H, Np),

- (8) (a) Zheng, L.; Miller, E. W.; Parlle, A.; Isacoff, E. Y.; Chang, C. J. *J. Am. Chem. Soc.* **2006**, *128*, 10–11. (b) Peng, X.; Du, J.; Fan, J.; Wang, J.; Wu, Y.; Zhao, J.; Sun, S.; Xu, T. *J. Am. Chem. Soc.* **2007**, *129*, 1500–1501. (c) Nolan, E. M.; Ryu, J. W.; Jaworski, J.; Feazell, R. P.; Sheng, M.; Lippard, S. *J. Am. Chem. Soc.* **2006**, *128*, 15517–15528.
- (9) (a) McClure, D. S. *J. Chem. Phys.* **1952**, *20*, 682–686. (b) Kavallieratos, K.; Rosenberg, J. M.; Chen, W. Z.; Ren, T. *J. Am. Chem. Soc.* **2005**, *127*, 6514–6515. (c) Praveen, L.; Ganga, V. B.; Thirumalai, R.; Sreeja, T.; Reddy, M. L. P.; Varma, R. L. *Inorg. Chem.* **2007**, *46*, 6277–6282.
- (10) (a) Kemlo, J. A.; Shepherd, T. M. *Chem. Phys. Lett.* **1977**, *47*, 158–162. (b) Ros-Lis, J. V.; Martínez-Máñez, R.; Rurack, K.; Sancenón, F.; Soto, J.; Spieles, M. *Inorg. Chem.* **2004**, *43*, 5183–5185. (c) Moon, S.-Y.; Youn, N. J.; Park, S. M.; Chang, S.-K. *J. Org. Chem.* **2005**, *70*, 2394–2397.
- (11) Chae, M.-Y.; Czarnik, A. W. *J. Am. Chem. Soc.* **1992**, *114*, 9704–9705.
- (12) (a) Mello, J. V.; Finney, N. S. *J. Am. Chem. Soc.* **2005**, *127*, 10124–10125. (b) Ono, A.; Togashi, H. *Angew. Chem., Int. Ed.* **2004**, *43*, 4300–4302. (c) Ros-Lis, J. V.; Marcos, M. D.; Martínez-Máñez, R.; Rurack, K.; Soto, J. *Angew. Chem., Int. Ed.* **2005**, *44*, 4405–4407.

7.20(d, 2H, Np). <sup>13</sup>C NMR (75 MHz, CDCl<sub>3</sub>), δ: 165.1, 162.1, 160.3, 135.4, 132.7, 132.1, 129.7, 129.5, 129.0, 128.3, 127.8, 127.6, 124.0, 121.9, 118.6, 108.6.

**Preparation of Fluorometric Metal-Ion Titration Solutions.** Emission spectra were recorded on an AMINCO Bowman Series 2 luminescence spectrometer. Fluorometric titration method was similar to that of UV-vis titration, and for all measurements excitation was at 430 nm. Both excitation and emission slit widths were 8 nm. Stock solutions (1.0 × 10<sup>-2</sup> mol/L) of the perchlorate or nitrate salts of Mn<sup>2+</sup>, Fe<sup>2+</sup>, Co<sup>2+</sup>, Ni<sup>2+</sup>, Zn<sup>2+</sup>, Cd<sup>2+</sup>, Pb<sup>2+</sup>, Hg<sup>2+</sup>, Cu<sup>2+</sup>, and the alkali and alkaline earth metal ions were prepared in aqueous solutions. Stock solutions of H<sub>2</sub>NB (1.0 × 10<sup>-5</sup> M) or Cu-NB (2.5 × 10<sup>-5</sup> M) were prepared in DMSO/H<sub>2</sub>O (4:1 v/v), respectively. Fluorescence quantum yield was determined using optically matching solution of Ru(2,2-bpy)<sub>3</sub>(ClO<sub>4</sub>)<sub>2</sub> (Φ<sub>f</sub> = 0.059 in CH<sub>3</sub>CN)<sup>13</sup> as standard at an excitation wavelength of 450 nm, and the quantum yield is calculated using eq 1,

$$\Phi_{\text{unk}} = \Phi_{\text{std}} \left( \frac{I_{\text{unk}}/A_{\text{unk}}}{I_{\text{std}}/A_{\text{std}}} \right) \left( \frac{\eta_{\text{unk}}}{\eta_{\text{std}}} \right)^2 \quad (1)$$

where Φ<sub>unk</sub> and Φ<sub>std</sub> are the radiative quantum yields of the sample and standard, I<sub>unk</sub> and I<sub>std</sub> are the integrated emission intensities of the corrected spectra for the sample and standard, A<sub>unk</sub> and A<sub>std</sub> are the absorbances of the sample and standard at the excitation wavelength (450 nm in all cases), and η<sub>unk</sub> and η<sub>std</sub> are the indices of refraction of the sample and standard solutions, respectively. Excitation and emission slit widths were modified to adjust the luminescent intensity in a suitable range. All of the spectroscopic measurements were performed at least in triplicate and averaged.

**Crystallography.** Intensities of H<sub>2</sub>NB and Cu-NB were collected on a Siemens SMART-CCD diffractometer with graphite-monochromated Mo Kα (λ = 0.71073 Å) using the SMART and SAINT programs.<sup>14</sup> Forty-five frames of data were collected at 298 K with an oscillation range of 1 deg/frame and an exposure time of 15 s/frame. Indexing and unit-cell refinement were based on all observed reflections from those 45 frames. The crystal data of H<sub>2</sub>NB and Cu-NB were listed in Table 1. The structures were solved by direct methods and refined on F<sup>2</sup> by full-matrix least-squares methods with SHELXTL version 5.1.<sup>15</sup> Non-hydrogen atoms were refined anisotropically with the exception of disordered solvent molecules. The acetonitrile molecules in Cu-NB were refined disordered into two parts with the site occupancy factors of the atoms being fixed at 0.5. Hydrogen atoms were fixed geometrically at calculated distances and allowed to ride on the parent non-hydrogen atoms with the isotropic displacement being fixed at 1.2 and 1.5 times that of the aromatic and methyl carbon atoms attached, respectively.

**Table 1.** Crystal Data for H<sub>2</sub>NB and Cu-NB

compound	H <sub>2</sub> NB	Cu-NB
molecular formula	C <sub>38</sub> H <sub>32</sub> Cl <sub>2</sub> N <sub>4</sub> O <sub>3</sub>	C <sub>38</sub> H <sub>27</sub> CuN <sub>5</sub> O <sub>2</sub>
fw	663.58	649.19
cryst syst	triclinic	triclinic
space group	P $\bar{1}$	P $\bar{1}$
a/Å	9.764(3)	10.909(2)
b/Å	12.480(5)	11.702(3)
c/Å	14.503(6)	13.553(3)
α/°	81.77(2)	99.904(4)
β/°	89.37(3)	91.971(4)
γ/°	76.03(2)	111.356(4)
V/Å <sup>3</sup>	1696.8(11)	1578.5(6)
Z	2	2
T/K	293	293
D <sub>calcd</sub> /Mgm <sup>-3</sup>	1.299	1.366
μ/mm <sup>-1</sup>	0.234	0.734
F(000)	692	670
no. reflns measured	10 092	7924
no. unique reflns (R <sub>int</sub> )	5742 (0.0484)	5451 (0.0867)
no. observed. reflns with I ≥ 2σ(I)	2958	2492
R1 <sup>a</sup>	0.0769	0.0655
wR2 <sup>a</sup>	0.2397	0.1573
GOF	1.030	1.055

$$^a R1 = \sum |F_o| - |F_c| / \sum |F_o|. wR2 = [\sum w(F_o^2 - F_c^2)^2 / \sum (F_o^2)]^{1/2}.$$

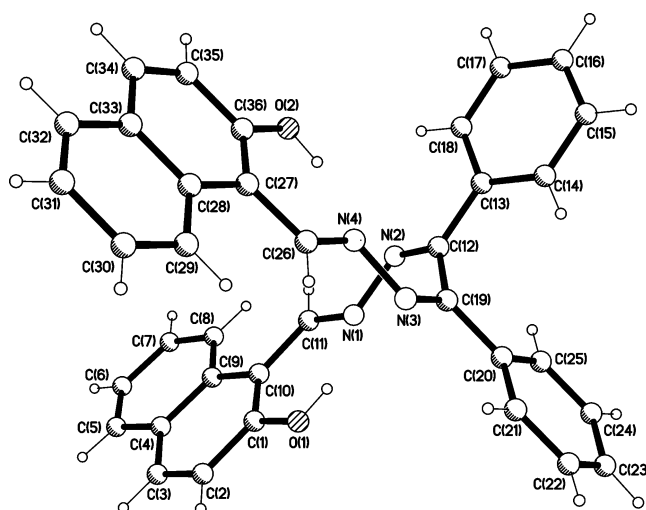


**Figure 1.** Molecular structure of ligand H<sub>2</sub>NB with the atomic numbering scheme. The solvent molecules were omitted for clarity. Distance and angles of selected bonds: C(1)–O(1) 1.348(3); C(36)–O(2) 1.333(3); C(11)–N(1) 1.278(3); N(1)–N(2) 1.403(3); N(2)–C(12) 1.283(3); C(19)–N(3) 1.288(3); N(3)–N(4) 1.401(3); N(4)–C(26) 1.276(3). C(11)–N(1)–N(2) 114.2(2); N(1)–N(2)–C(12) 112.8(2); C(19)–N(3)–N(4) 112.8(2); N(3)–N(4)–C(26) 111.9(2).

## Results and Discussion

**Optical Properties and Cu<sup>2+</sup>-Specific Responses of H<sub>2</sub>NB.** The Schiff-base ligand H<sub>2</sub>NB was prepared by the reaction of benzil dihydrazone with 2-hydroxy-1-naphthalene-carboxaldehyde in a methanol solution and identified by the single crystal X-ray structural analysis. As shown in Figure 1, the two naphthol rings position on opposite sides of the N(2)–C(12)–C(19)–N(3) fragment, giving rise to a helix similar to that observed in the related ligand, N,N'-bis[1-(pyrazine-2-yl)ethylidene]benzil dihydrazone.<sup>16</sup> The helix twisted in the ligand mainly arises

(13) Juris, A.; Balzani, V. *Coord. Chem. Rev.* **1988**, *84*, 85–277.  
 (14) SMART and SAINT, Area Detector Control and Integration Software; Siemens Analytical X-ray Systems, Inc.: Madison, WI, 1996.  
 (15) Sheldrick, G. M. *SHELXTL V5.1, Software Reference Manual*; Bruker, AXS, Inc.: Madison, WI, 1997.

(16) Bai, Y.; Duan, C. Y.; Cai, P.; Dang, D. B.; Meng, Q. J. *Dalton Trans.* **2005**, 2678–2680.

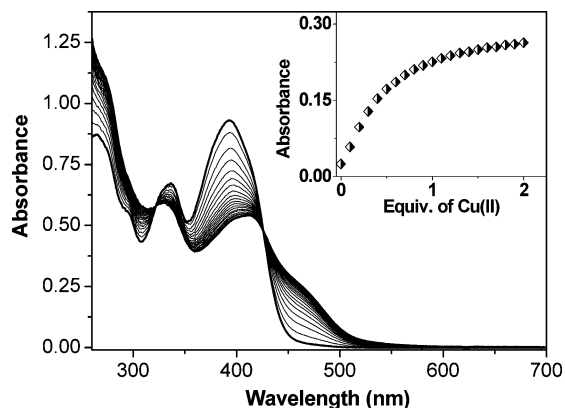


**Figure 2.** UV-vis titration of  $\text{H}_2\text{NB}$  ( $10 \mu\text{M}$ ) in  $\text{DMSO}/\text{H}_2\text{O}$  (4:1 v/v) solution upon addition of  $\text{Cu}^{2+}$ . Inset: UV-vis titration profile of  $\text{H}_2\text{NB}$  upon addition of  $\text{Cu}^{2+}$ ; the absorption is recorded at 460 nm.

from the torsion around the N-C-C-N bond with an angle of  $103^\circ$ .

The UV-vis absorption spectrum (Figure 2) of the ligand  $\text{H}_2\text{NB}$  in a  $\text{DMSO}/\text{H}_2\text{O}$  (4:1 v/v) solution exhibited a broad naphthol-based  $\pi-\pi^*$  transition band around 393 nm. Upon the addition of a  $\text{Cu}(\text{ClO}_4)_2 \cdot 6\text{H}_2\text{O}$  aqueous solution, a new band centered around 460 nm appeared. The absorption increased almost linearly with the ratio of  $[\text{Cu}^{2+}]/[\text{ligand}]$  until the first stoichiometry. Meanwhile, the absorption band of 393 nm fell down to a limit value and had a slight redshift. The presence of well-defined isosbestic points at 425 and 325 nm indicated that only two species coexisted in the equilibrium. Job's plot evaluated from the absorption spectra of the titration solution (Supporting Information Figure S1) exhibited the inflection point at 0.5, indicating the formation of a 1:1  $\text{H}_2\text{NB}-\text{Cu}(\text{II})$  complexation species in the solution; and the linear fitting<sup>17</sup> of the titration curve at 460 nm based on a 1:1 stoichiometry host-guest mode (Supporting Information Figure S2) gave an association constant ( $\log K_{\text{ass}}$ ) of  $5.20 \pm 0.1$ . Similar measurements for several other metal ions were carried out. However, the changes of the UV spectra could scarcely be observed even if these metal cations were added up in 10-fold amounts of  $\text{Cu}^{2+}$  under the same conditions, indicating that the UV-vis response of  $\text{H}_2\text{NB}$  is  $\text{Cu}^{2+}$  specific.

$\text{H}_2\text{NB}$  exhibited an emission band centered about 530 nm (quantum yield  $\Phi \approx 0.080$ ) in  $\text{DMSO}/\text{H}_2\text{O}$  (4:1 v/v) (Figure 3) when excited at 430 nm (near one of the two isosbestic points in the absorption spectrum).<sup>18</sup> Upon the addition of 1 equiv of  $\text{Cu}^{2+}$  ions, the fluorescence was quenched significantly. The association constant of the  $\text{Cu}^{2+}$ -ligand complexation species ( $\log K_s = 5.44 \pm 0.1$ ) calculated from the fluorescence titration measurements was consistent well with the value derived from UV-vis titration study, indicating a strong tendency to form the  $\text{Cu}^{2+}$ -ligand complexation species. When  $0.25 \mu\text{M}$  of  $\text{Cu}^{2+}$  was added to the solution of  $\text{H}_2\text{NB}$  ( $1 \mu\text{M}$ ), a fluorescence decrease of 10% is observed,

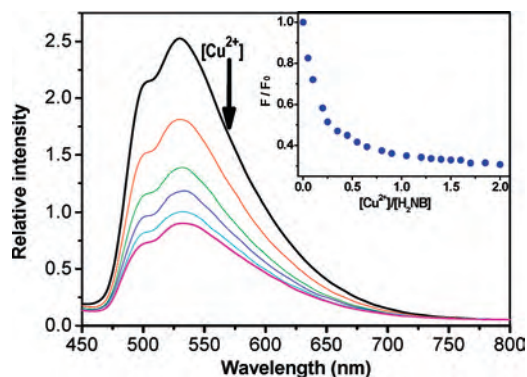


**Figure 3.** Fluorescence emission spectra of the ligand  $\text{H}_2\text{NB}$  ( $10 \mu\text{M}$ ) in 2 mL  $\text{DMSO}/\text{H}_2\text{O}$  (4:1 v/v) with successive addition of  $\text{Cu}^{2+}$ . The curves of 0, 0.2, 0.4, 0.6, 0.8, and 1.0 equiv of added  $\text{Cu}^{2+}$  were shown. The insert exhibits a fluorescence titration profile at 530 nm upon the addition of  $\text{Cu}^{2+}$  (excitation at 430 nm).

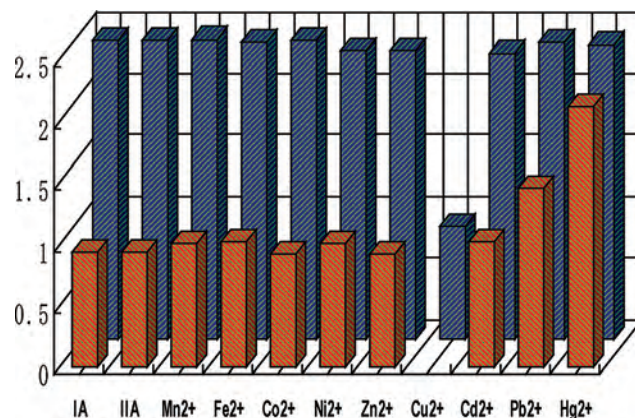


**Figure 4.** Fluorescence responses of  $\text{H}_2\text{NB}$  ( $10 \mu\text{M}$ ) to various cations in  $\text{DMSO}-\text{H}_2\text{O}$  (4:1 v/v) solution. The blue bars represent the emission intensities of  $\text{H}_2\text{NB}$  in the presence of 0.10 mM of alkali (IA) and alkaline earth (IIA) metals and for other cations of interest. The orange bars represent the change of the emission that occurs upon the subsequent addition of 0.01 mM of  $\text{Cu}^{2+}$  to the above solution. The intensities were recorded at 530 nm, excitation at 430 nm.

indicating that the detection limit of  $\text{H}_2\text{NB}$  to  $\text{Cu}^{2+}$  is at the nanomolar level.

Compound  $\text{Cu}-\text{NB}$  was isolated from the reaction of ligand  $\text{H}_2\text{NB}$  with copper perchlorate. An X-ray structural investigation revealed that  $\text{Cu}-\text{NB}$  exhibited a mononuclear structure with the  $\text{Cu}^{2+}$  center coordinated by two imine nitrogen atoms and two naphthol oxygen atoms in a distorted square geometry (Figure 5). The twisted angle of the two chelating rings was calculated as  $139^\circ$ . The ligand lost two protons from the two naphthol groups and coordinated to  $\text{Cu}^{2+}$  as a dianionic  $\text{N}_2\text{O}_2$  tetradentate chelator, which was confirmed by the C-O bond distances of 1.28 Å. The N(2)-C(12)-C(19)-N(3) torsion angle is  $82.6^\circ$ . Such a special twisted conformation of  $\text{H}_2\text{NB}$  in the molecule, combined with a high thermodynamic affinity to typical *N,O*-chelate ligands and fast metal-to-ligand binding kinetics of  $\text{Cu}^{2+}$ , would be expected to lead a larger association of the  $\text{Cu}-\text{NB}$  constant than that of most the first-row transition-metal ions.<sup>19</sup>

The fluorescent spectra of  $\text{H}_2\text{NB}$  using the other divalent metal ions instead of  $\text{Cu}^{2+}$  were recorded. The results showed that the fluorescent intensity of  $\text{H}_2\text{NB}$  was hardly affected

(17) Lin, Z.-H.; Xie, L.-X.; Zhao, Y.-G.; Duan, C.-Y.; Qu, J.-P. *Org. Biomol. Chem.* **2007**, *5*, 3535-3538.

(18) Zhang, B.-G.; Xu, J.; Zhao, Y.-G.; Duan, C.-Y.; Cao, X.; Meng, Q.-J. *Dalton. Trans.* **2006**, 1271-1276.

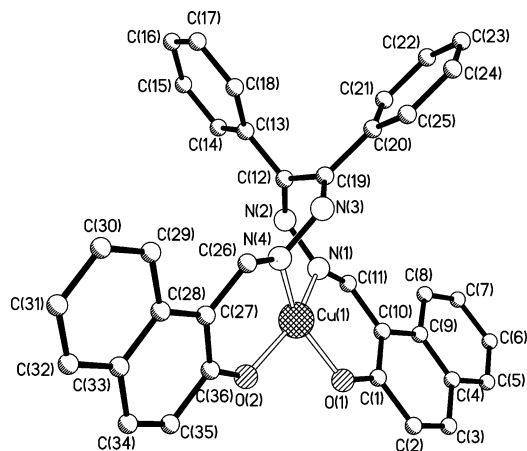


**Figure 5.** Molecular structure of compound Cu–NB with the atomic numbering scheme. Hydrogen atoms and the acetonitrile molecule were omitted for clarity. Distance (Å) and angles (°) of selected bonds: Cu(1)–O(2) 1.886(4), Cu(1)–O(1) 1.865(4); Cu(1)–N(1) 1.956(5), Cu(1)–N(4) 1.932(5), N(1)–C(11) 1.282(7); N(4)–C(26) 1.276(7); C(36)–O(2) 1.279(6); C(1)–O(1) 1.280 (7). O(1)–Cu(1)–N(1) 91.8(2). O(1)–Cu(1)–O(2) 91.8(2), O(1)–Cu(1)–N(4) 150.4(2), O(2)–Cu(1)–N(4) 90.8(2), O(1)–Cu(1)–N(1) 91.8(2), O(2)–Cu(1)–N(1) 155.6(2), N(4)–Cu(1)–N(1) 97.9(2).

by these ions even up to the 10-fold amounts of the ligand, which was also in good agreement with the UV–vis results. The high selectivity of H<sub>2</sub>NB for Cu<sup>2+</sup> over other metal ions should be in part contributed to the strong coordination ability of Cu<sup>2+</sup> and its large association constant. To further investigate the selectivity of H<sub>2</sub>NB as a luminescence sensor for the detection of Cu<sup>2+</sup>, competitive experiments were carried out. As shown in Figure 5, upon the addition of 0.1 mM of Mn<sup>2+</sup>, Fe<sup>2+</sup>, Co<sup>2+</sup>, Ni<sup>2+</sup>, Zn<sup>2+</sup>, Cd<sup>2+</sup>, Pb<sup>2+</sup>, Hg<sup>2+</sup>, and alkali and alkaline earth metal ions to the solutions of H<sub>2</sub>NB (10 μM), no significant fluorescence changes were observed. Upon the addition of Cu<sup>2+</sup> (10 μM) to the above-mentioned solutions, fluorescence intensities of these solutions except Hg<sup>2+</sup> immediately dropped down to the level of that for the H<sub>2</sub>NB solution containing only a Cu<sup>2+</sup> (10 μM) ion. Thus, the coexistence of 0.1 mM of Mn<sup>2+</sup>, Fe<sup>2+</sup>, Co<sup>2+</sup>, Ni<sup>2+</sup>, Zn<sup>2+</sup>, Cd<sup>2+</sup>, Pb<sup>2+</sup>, and the alkali and alkaline earth metal ions also did not impact the Cu<sup>2+</sup>-binding quenching. Only the presence of Hg<sup>2+</sup> could block the quenching process of Cu<sup>2+</sup>. It was thus expected that, upon the displacement of the Cu<sup>2+</sup> by Hg<sup>2+</sup>, Cu<sup>2+</sup> would no longer participate in the quenching process; the recovery of the fluorescence of the ligand would be achieved.

**Optical Properties and Hg<sup>2+</sup>-Specific Responses of Cu–NB.** The UV–vis absorption spectrum of Cu–NB in DMSO/H<sub>2</sub>O (4:1 v/v) exhibited a metal-to-ligand charge transfer (MLCT) band around 460 nm. Upon the addition of a aqueous solution of Hg(ClO<sub>4</sub>)<sub>2</sub>, the MLCT band decreased continuously accompanied with the appearance of a new peak at 393 nm, corresponding to the π–π\* transition of naphthol groups (Figure 6). The presence of two well-defined isosbestic points coupled with the sigmoidal shape of the titration curve suggested a one-step reaction. Meanwhile, the addition of other metal ions such as Co<sup>2+</sup>, Ni<sup>2+</sup>, Zn<sup>2+</sup>, Cd<sup>2+</sup>, Pb<sup>2+</sup>, and alkali and alkaline earth metal ions did not cause any obvious spectral changes, even in 10-fold excess. The high selectivity of the Cu–NB for Hg<sup>2+</sup> over

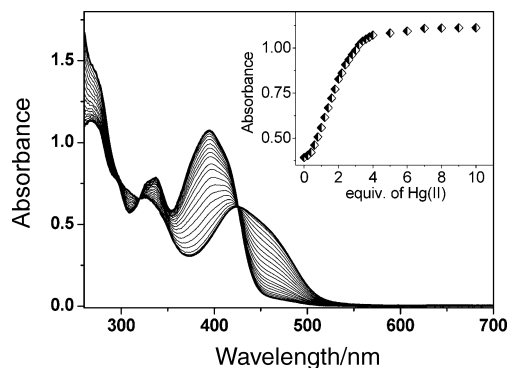


**Figure 6.** UV–vis titration of Cu–NB (10 μM) in DMSO/H<sub>2</sub>O (4:1 v/v) solution upon the addition of Hg<sup>2+</sup>. Inset: Titration curve of the absorbance intensity at 393 nm as a function of the ratio of [Hg<sup>2+</sup>]/[Cu–NB].

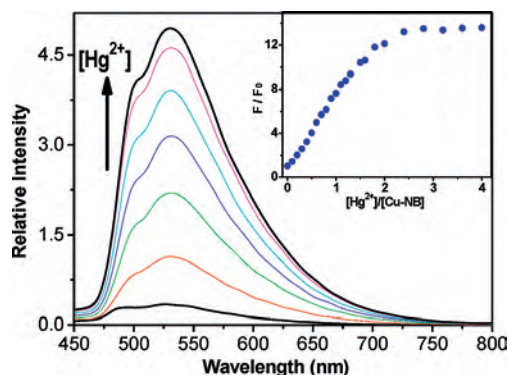


**Figure 7.** Luminescent titration of compound Cu–NB (25 μM) upon addition of Hg<sup>2+</sup>. Excitation at 430 nm in DMSO/H<sub>2</sub>O (4:1 v/v) solution. The insert exhibits the fluorescence titration profile of Cu–NB at 530 nm upon addition of Hg<sup>2+</sup>.

other metal ions should be in part contributing to the strong coordination ability of Cu<sup>2+</sup> and its large association constant.

When excited at 430 nm, Cu–NB exhibited a very weak luminescence band at about 530 nm corresponding to the typical emission of the naphthol rings.<sup>18</sup> The low luminescent intensity is likely to result from the quenching of emission by Cu<sup>2+</sup> through a PET mechanism and/or a paramagnetic quenching mechanism.<sup>20</sup> As shown in Figure 7, the addition of Hg(ClO<sub>4</sub>)<sub>2</sub> caused a dramatic immediate increase in emission intensity up to the maximum (Φ ≈ 0.081). These results combined with the sigmoidal shape of the titration curve suggested that of the Cu<sup>2+</sup> ion in the Cu–NB complex was substituted by Hg<sup>2+</sup>. According to the two titration curves, the association constant log K<sub>ass</sub> of the mercury coordination species was calculated as 6.12 ± 0.1, larger than that of the Cu<sup>2+</sup> complex. In addition, the profiles of UV–vis and luminescent spectra of Cu–NB in the presence of Hg<sup>2+</sup> were quite similar to that of the free ligand. The emission intensity at 530 nm (excited at 430 nm) was enhanced to 10% of the original intensity of Cu–NB (1 μM) when 250 nM (or 50 ppb) Hg<sup>2+</sup> was added to the solution, indicating that the limit

(19) (a) Krämer, R. *Angew. Chem., Int. Ed* **1998**, *37*, 772–773. (b) Fabbrizzi, L.; Licchelli, M.; Pallavicini, P.; Perotti, A.; Taglietti, A.; Sacchi, D. *Chem.–Eur. J.* **1996**, *2*, 75–82. (c) Fabbrizzi, L.; Licchelli, M.; Pallavicini, P.; Perotti, A.; Sacchi, D. *Angew. Chem., Int. Ed. Engl.* **1994**, *33*, 1975–1977.

(20) Varnes, A. W.; Dodson, R. B.; Wehry, E. L. *J. Am. Chem. Soc.* **1972**, *94*, 946–950.

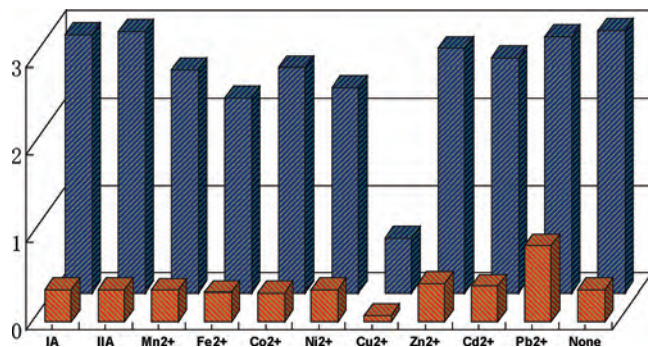


**Figure 8.** Fluorescence responses of Cu–NB (25  $\mu\text{M}$ ) to various cations in DMSO/H<sub>2</sub>O (4:1 v/v) solution. The blue bars represent the emission intensities of Cu–NB in the presence of 0.25 mM of alkali (IA) and alkaline earth (IIA) metals and for other cations of interest. The orange bars represent the change of the emission that occurs upon the subsequent addition of 0.05 mM of Hg<sup>2+</sup> to the above solution. The intensities were recorded at 530 nm, excitation at 430 nm.

of detection of Cu–NB to Hg<sup>2+</sup> met the discharge limit for industrial wastewater according to the U.S. EPA standard,<sup>21</sup> or China SA standard.<sup>22</sup>

To further explore the availability of Cu–NB as a highly selective probe for Hg<sup>2+</sup>, the fluorescent spectra of Cu–NB coexisting with the other metal ions that could probably affect the fluorescence were examined. When solutions of Cu–NB (25  $\mu\text{M}$ ) were respectively added, 10 equivalents of Mn<sup>2+</sup>, Fe<sup>2+</sup>, Co<sup>2+</sup>, Ni<sup>2+</sup>, Zn<sup>2+</sup>, Cd<sup>2+</sup>, and the alkali or alkaline earth metal ions (0.25 mM), no obvious changes in the fluorescent spectra were observed other than Pb<sup>2+</sup> showing a marginal alteration. Adding 50  $\mu\text{M}$  equivalent of Hg<sup>2+</sup> to the above solutions gave rise to drastic increments of their fluorescence intensities, revealing that Hg<sup>2+</sup> could have specific effects on the luminescence spectra, and the Hg<sup>2+</sup>-specific responses were not disturbed by the competitive ions (Figure 8). The results strongly suggested that Cu–NB could be used as a selective sensor for mercuric ion. In principle, this method offers a general approach for the fluorescence detection of metal ions, which show poor selectivity when the metal ions are directly attached to the sensor.

Of course, the presence of Cu<sup>2+</sup> could influence the detection of Hg<sup>2+</sup> in the solution. By adding an incremental amount of Cu<sup>2+</sup> ions, the UV–vis and luminescent spectra of the Hg–ligand system were gradually recovered into the profiles of the spectra of the Cu–NB system. However, the reaction did not reach its full equilibrium even when 10 times excess of Cu<sup>2+</sup> were added, which confirmed that Hg–H<sub>2</sub>NB complexation species has higher stability than the Cu–NB complexation species. Meanwhile, the competitive Hg<sup>2+</sup>/Cu<sup>2+</sup> off–on–off-type fluorescent signal control is reminiscent of the Ca<sup>2+</sup>/K<sup>+</sup> induced chromogenic behavior of a calix-crown-5 derivative containing an indoaniline chromophore<sup>23</sup> and has been observed in a fluoroionophore-based cyclam system.<sup>24</sup>

**The Mechanism Study of the Displacement Approach.** From a mechanistic viewpoint, the d<sup>10</sup> configuration of Hg<sup>2+</sup> with tetrahedral coordination geometry, and a large ionic radius is likely to take advantage of the specific binding to the ligand having two closed naphthol rings. Whereas the tetrahedrally distorted coordination geometry constrained by the ligand prevented the first-row transition-metal ions from more strongly binding to the ligand than Cu<sup>2+</sup> does, the Hg<sup>2+</sup> ions could be readily substituted for d<sup>9</sup> electronic conformation Cu<sup>2+</sup>, leading to the blocking of the quenching channel and achieving the recovery of the initial luminescence in the on state with high selectivity.<sup>25</sup> A solid evidence for the displacement reaction came from the ESI-MS spectrum (Figure 9). Whereas the neutral Cu–NB itself did not exhibit any observable positive peak at *m/z* ranging from 500 to 1000 in ESI-MS spectrum, upon the addition of Hg<sup>2+</sup> a peak at *m/z* = 746.7 corresponding to the [Hg(HNB)]<sup>+</sup> species appeared. The isotopic peak of the original peak fit very well to the isotope distribution pattern calculated with the *IsoPro 3.0* program for [Hg(HNB)]<sup>+</sup>.

To further look into the nature of the interaction between H<sub>2</sub>NB and the Hg<sup>2+</sup> ion, pure Hg<sup>2+</sup>–H<sub>2</sub>NB complex was isolated and characterized. Compared to the <sup>1</sup>H NMR spectrum of the free ligand H<sub>2</sub>NB, the Hg<sup>2+</sup> binding caused the small but significant downfield shifts of almost all of the proton signals (Figure 10). Especially for the protons in the naphthol ring, 0.25 ppm for H<sub>5</sub> and 0.17 for H<sub>3</sub>, and so forth, strongly suggested the participation of the naphthol rings in the coordination.<sup>26</sup> The presence of broadband at about 12.9 ppm comparing to that of 12.5 ppm in the spectrum of H<sub>2</sub>NB demonstrated the existence of OH protons during Hg<sup>2+</sup> binding.

**Electrochemical Responses of Cu–NB to Hg<sup>2+</sup>.** Cu–NB exhibited a Cu<sup>2+</sup>/Cu<sup>+</sup> redox couple at about –595 mV of a differential pulse voltammetric (DPV) measurement in a DMSO/H<sub>2</sub>O (4:1 v/v) solution (Figure 11). Such a reversible redox response could provide another opportunity for Cu–NB to act as a multisignaling sensor for Hg<sup>2+</sup>. Adding Hg<sup>2+</sup> caused the current of the peak at –595 mV decreased with the potential anodically shifted, indicating that the displacement reaction could occur with the concentration of the copper compound Cu–NB decreased and the free Cu<sup>2+</sup> increased. Meanwhile, new peaks at about –90 and 45 mV appeared and developed. The former peak was assigned to the Hg<sup>2+</sup> complex couple, which increased and anodically shifted with the increasing of Hg<sup>2+</sup>, the latter was attributed to the redox potential of the Cu<sup>2+</sup>/Cu<sup>+</sup> couple without binding to the ligand. Clearly, the presence of Hg<sup>2+</sup> caused the potential of Cu<sup>2+</sup>/Cu<sup>+</sup> anodically shifted about 640 mV. Consequently, both the current intensity and the potential of the peak around –595 mV could be used to monitor the concentration of Cu–NB. More interestingly, no perturbation

(21) *Regulatory Impact Analysis of the Clean Air Mercury Rule*; U.S. EPA: Research Triangle Park, NC, 2005; EPA-452/R-05-003.

(22) Standardization Administration (SA) of the People's Republic of China, Integrated Wastewater Discharge Standard, GB 8978, 1996.

(23) Kubo, Y.; Obara, S.; Tokita, S. *Chem. Commun.* **1999**, 2399–2400.

(24) Kim, S. H.; Kim, J. S.; Park, S. M.; Chang, S. K. *Org. Lett.* **2006**, 8, 371–374.

(25) Valeur, B.; Leray, I. *Coord. Chem. Rev.* **2000**, 205, 3–40.

(26) (a) Wang, J. B.; Qian, X. H. *Chem. Commun.* **2006**, 109–111. (b) Shiraiishi, Y.; Maehara, H.; Ishizumi, K.; Hirai, T. *Org. Lett.* **2007**, 9, 3125–3128.

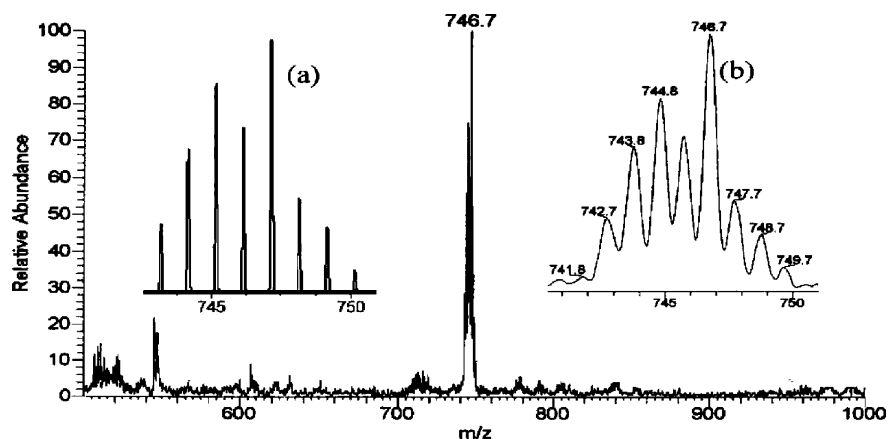


**Figure 9.** ESI-MS spectrum of the Cu–NB (2 mM) in DMSO/H<sub>2</sub>O (4:1 v/v) solution upon addition of Hg<sup>2+</sup> (5 mM). Inserts are (a) the result of the IsoPro 3.0 ESI-MS spectrum simulation program and (b) the experimental measurement.

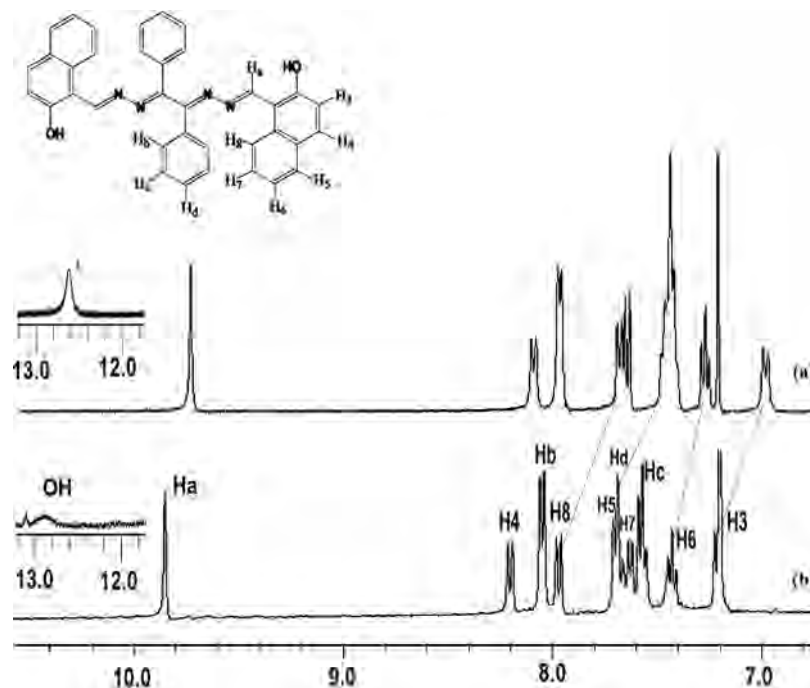


**Figure 10.** <sup>1</sup>H NMR spectra solution of the free H<sub>2</sub>NB ligand, the hydrogen atoms with various chemical shifts are ascribed (a) and the Hg<sup>2+</sup> complex (b), in CDCl<sub>3</sub>.

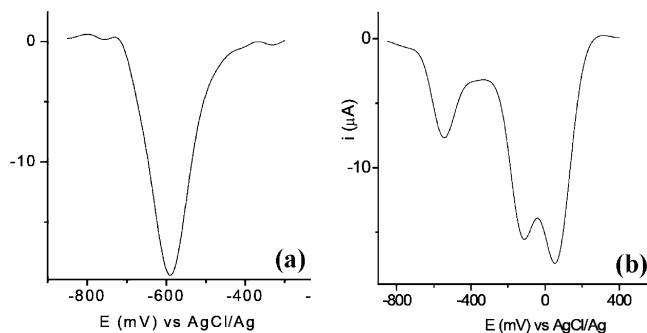


**Figure 11.** DPV of Cu–NB (1 mM in DMSO solution, 0.1 M *n*-Bu<sub>4</sub>NClO<sub>4</sub>) (a) and in the presence of 1 mM ratio of Hg(ClO<sub>4</sub>)<sub>2</sub> in DMSO/H<sub>2</sub>O (4:1 v/v) solution.

of the DPV of Cu–NB was observed upon the addition of Na<sup>+</sup>, K<sup>+</sup>, Ca<sup>2+</sup>, Mg<sup>2+</sup>, Ni<sup>2+</sup>, Co<sup>2+</sup>, Zn<sup>2+</sup>, Cd<sup>2+</sup>, and even Pb<sup>2+</sup> metal ions; such that the larger separation (640 mV) of the redox potential of Cu<sup>2+</sup>/Cu<sup>+</sup> clearly reveals that the Cu–NB

could also be operated as a highly selective and sensitive electrochemical sensor for Hg<sup>2+</sup> over other metal ions, besides the fluorometric response for Hg<sup>2+</sup>. The redox titration of the free ligand with Hg<sup>2+</sup> exhibited a peak at about –80 mV, which was developed and anodically shifted. It was assigned to the Hg<sup>2+</sup>/Hg<sup>+</sup> couple of the ligand–Hg<sup>2+</sup> complexation species.

### Conclusions

In summary, we have demonstrated a new and broadly applicable displacement approach to identify new fluorescent chemosensors. The experiments show that using the metal complex rather than organic dyes as a luminescent probe for cations could effectively avoid the interference of other metal cations with weaker binding capability and that the naphtholate/naphthol-based off–on signaling mode is more beneficial than the on–off-type transductions. The discovery of this new Hg<sup>2+</sup>-responsive chemosensor with

high selectivity even in the presence of excess mono/divalent ions and other contaminants reflects the validity of this approach and proves the hypothesis that the displacement signaling mechanism is suitable to such an exploration. Hopefully, this preliminary understanding of this cation-sensing mechanism would be helpful to find new practical probes that show excellent cation-sensing capacity in water or at least in water-containing organic solvents through structural modification.

**Acknowledgment.** This work is supported by the National Natural Science Foundation of China and the Start-Up Fund of Dalian University of Technology.

**Supporting Information Available:** Additional spectroscopic data and CIFs of ligand **H<sub>2</sub>NB** and Cu-**NB**. This material is available free of charge via the Internet at <http://pubs.acs.org>.

IC702494S